Preparation, structure, and properties of the superconducting compound series $Bi_2Sr_2Ca_{n-1}Cu_nO_y$ with $n=1$, 2, and 3

J. M. Tarascon
Bellcore, 331 Newman Springs Road, Red Bank, New Jersey 07701

W. R. McKinnon
National Research Council, Division of Chemistry, Ottawa, Canada K1A0R9

P. Barboux, D. M. Hwang, B. G. Bagley, L. H. Greene, and G. W. Hull
Bellcore, 331 Newman Springs Road, Red Bank, New Jersey 07701

Y. LePage
National Research Council, Division of Chemistry, Ottawa, Canada K1A0R9

N. Stoffel and M. Giroud
Bellcore, 331 Newman Springs Road, Red Bank, New Jersey 07701
(Received 18 May 1988; revised manuscript received 26 August 1988)

Crystals of the three Bi-based cuprates of general formula $Bi_2Sr_2Ca_{n-1}Cu_nO_y$ with $n=1$, 2, and 3 have been isolated and their structural and physical properties investigated. The structures are similar, differing only in the number of CuO_2-Ca-CuO_2 slabs packed along the c axis. The insertion of one and two slabs increases c from 24.6 to 30.6 and 37.1 Å. Transmission electron microscopy shows there are stacking faults within the crystals in agreement with our x-ray data and its analysis. Resistivity, ac susceptibility, and dc magnetization measurements demonstrate superconductivity in the $n=1$, 2, and 3 phases at 10, 85, and 110 K, respectively. The observed transition temperatures and the stacking fault densities are dependent upon sample processing, in particular, the annealing temperatures and cooling rates. The transition temperature is, within the accuracy of our chemical titration, independent of the average copper valency that was determined to be 2.15 ± 0.03 for each of the three compounds.

I. INTRODUCTION

Since the discovery by Bednorz and Müller[1] of high transition temperature (T_c) superconductivity in the oxides and the achievement of $T_c=90$ K by Wu *et al.*,[2] these new materials have all contained either La or a rare earth as a principal constituent. Recently, superconductivity at 20 K was reported by Michel *et al.* for the Bi-Sr-Cu-O system.[3] The addition of Ca to this ternary led Maeda, Tanaka, Fukutumi, and Asano[4] to the discovery of bulk superconductivity at 85 K and evidence of superconductivity at 110 K in the Bi-Sr-Ca-Cu-O system. Since this initial discovery, there have been many publications detailing the existence of superconductivity at $T \cong 110$ K, and discussing the structure of compounds of the form Bi-Sr-Ca-Cu-O.[5-11] The compound of formula $Bi_4Sr_3Ca_3Cu_4O_{16}$ (hereafter denoted 4:3:3:4) was found to be responsible for superconductivity at 85 K in the Bi system and its structure established.[12,13] The crystal substructure can be viewed as a three-dimensional packing of $Bi_2Sr_2Ca_1Cu_2O_8$ slabs along the c axis, with the main feature being the presence of two Bi-O layers separated by 3.0 Å and shifted, with respect to each other (crystallographic shear) along the diagonal direction of the perovskite subcell. Within this class of compounds, Bi can be replaced by thalium and new phases of general formula $Tl_2Ba_2Ca_{n-1}Cu_nO_y$ ($n=1$, 2, and 3) have been isolated.[14-16] The thallium substitution does not significantly affect the structure, which is tetragonal with a double layer of Tl-O separated by 2.6 Å, but does raise T_c to 125 K when $n=3$.[16] In contrast to the thallium phases, which are easy to form independent of n, difficulties have been encountered in the preparation of the homologue Bi phases, particularly the 110-K phase. We previously[17] measured zero resistance at 107 K on Bi pseudomorphs of composition 2:2:2:3, but were not able to determine the structure because of the absence of long-range structural order. However, the presence of a larger c axis for the 110 K was evidenced by the presence of a Bragg peak located at $2\theta=4.6°$ in the x-ray powder pattern of a multiphase sample showing both 85- and 110-K superconducting transitions. We report here the synthesis of the $Bi_2Sr_2Ca_{n-1}Cu_nO_y$ phases with $n=1$, 2, and 3 and on the relationship between their structural and physical properties. We show evidence that the 110-K phase has the 2:2:2:3 formula and, furthermore, that its structure contains three CuO_2 layers with the possibility for stacking faults. For clarity, we present the synthesis and physical measurements for each phase separately and comment on their interrelationships in the discussion section.

II. SYNTHESIS AND STRUCTURE OF THE $Bi_2Sr_2Ca_{n-1}Cu_nO_y$ PHASES

A. $n=1$

Michel *et al.*[3] reported superconducting critical temperatures ranging from 10 to 20 K for the Bi-Sr-Cu-O system and attributed superconductivity to the $Bi_2Sr_2Cu_2O_7$ phase, whereas a different phase ($Bi_2Sr_2CuO_6$) was proposed by two other groups.[18,19] However, all agree that the T_c of the resulting material is strongly dependent on sample processing. We observe, for example, that depending upon whether the sample is heated below or above its melting point produces marked differences in the resulting physical properties.

$Bi_2Sr_2CuO_6$ (2:2:0:1) was prepared by firing, at high temperatures, stoichiometric amounts of Bi_2O_3, $SrCO_3$, or SrO_2, and CuO powders (each 99.999% pure). Three heating processes were investigated: (1) the mixed powders (using $SrCO_3$) were fired at temperatures ranging from 840–880 °C for several days and then furnace cooled to room temperature (samples denoted as *P*); (2) the mixed powders (using $SrCO_3$) were melted at 1100 °C for 2 h, the temperature was lowered to 890 °C and held there for several days, then the samples were furnace cooled (samples denoted as *M*); (3) SrO_2 was used as the Sr oxide precursor, and pressed pellets were placed on alumina, sealed in quartz tubes, and reacted for 15 h at 870 °C (samples denoted as *Q*). The *M* samples, depending on the cooling rate from 1100 to 890 °C, may exhibit either large plateletlike crystals radiating out of the bulk (4 h cool) or an acicular structure (furnace cooled). This is common for layered-type materials. For example graphite, which has a lamellar structure, can also be made in a fiber form (graphite fibers). Both *M* and *P* samples contain a few percent of a second phase, but the *Q* samples are single phase. In all three cases, the Bragg peaks of the majority phase can be completely indexed on a pseudotetragonal unit cell with lattice parameters $a=5.39$ Å and $c=24.6$ Å. The experimental agreement in the lattice parameters for samples *Q* (prepared in sealed tubes) with those of samples prepared in open containers shows that there is little or no Bi lost from the open containers during the reaction.

Although the *M* samples contain a second phase, that phase is not present in plateletlike crystals picked from the *M* samples. Figure 1(a) shows the x-ray diffraction pattern of such crystals. Because the crystals are oriented (as we found before[12]), only the [00*l*] reflections appear. The plateletlike crystals have a composition 2:2:0:1, as determined by Rutherford backscattering spectrometry (RBS) (see Fig. 2).

Transmission electron microscopy (TEM) on crushed (2:2:0:1) crystals reveals lattice parameters similar to those determined by x-ray diffraction with, in addition, an incommensurate superstructure along the [0*k*0] direction. A TEM micrograph is shown in Fig. 3(a). Note that in the [00*l*] direction there is a Bi-O double layer repeat distance of 12.3 Å. Because of the crystallographic shear in Bi layers, this leads to a *c* parameter of $2\times12.3=24.6$ Å. These results agree with those reported by Torardi *et al.*[19] for the $Bi_2Sr_2CuO_6$ phase containing one CuO_2 layer.

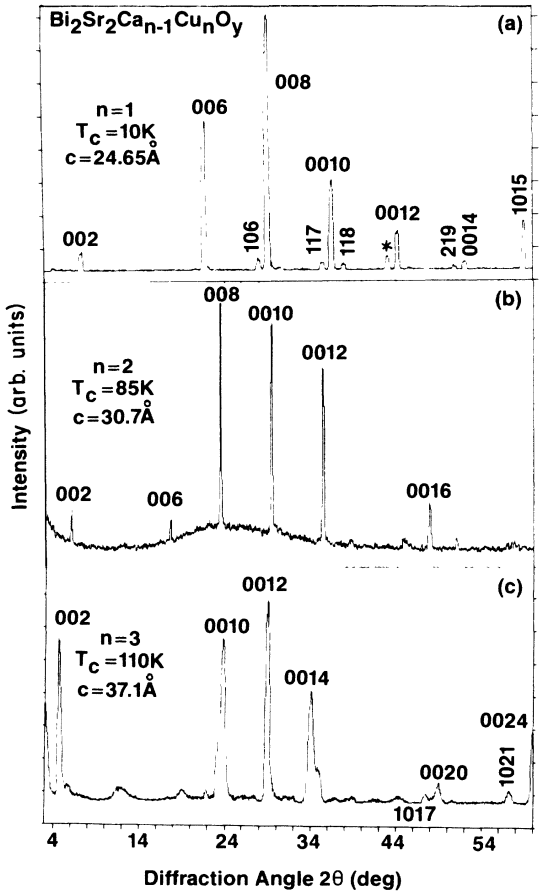

FIG. 1. The x-ray diffraction patterns for highly *c*-oriented multicrystalline samples of the three Bi phases are shown with the Miller indices above each peak. Note that only the [00*l*] reflections with *l* even are observed. Resolution has been decreased in order to increase the intensity of the Bragg peaks in (a) and (c).

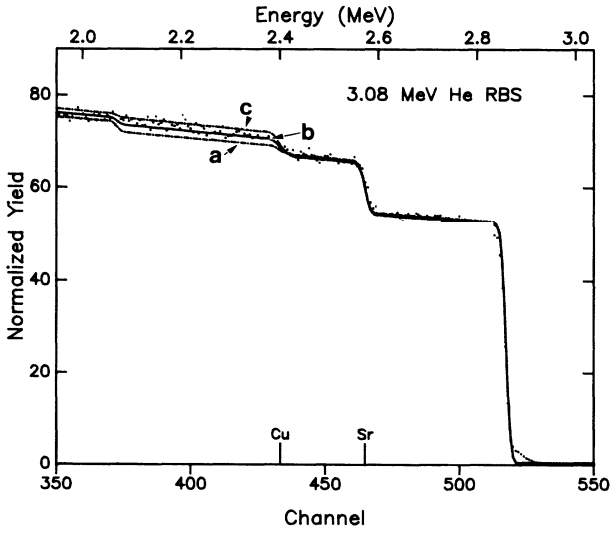

FIG. 2. RBS measurement of a $Bi_4Sr_4Cu_2O_y$ crystal prepared from the melt (see text). The simulation for one, two, and three Cu are shown by curves a, b, and c, respectively.

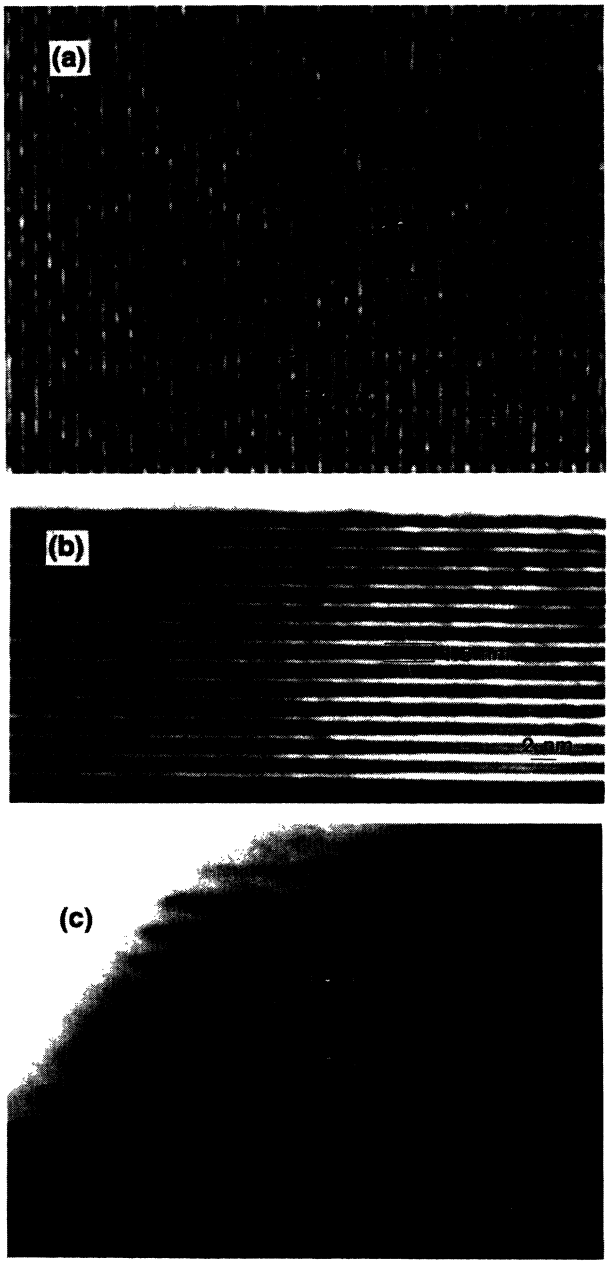

FIG. 3. Crushed powders of the three types of samples were examined using a JEOL 4000FX transmission electron microscope. (a) TEM lattice image of the 10-K material along the [100] direction. The double dark layers are assigned as the double Bi-O layers. The doubling of the unit cell due to the shearing of the Bi layers is delineated by the interweaving appearance of this micrograph. (b) Bright-field TEM image of the 85-K material showing uniform c-layer spacing of 15.4 Å. (c) Bright-field TEM image of the 110-K material showing imperfect order in the c direction. The observed c-layer spacing is usually 19 Å. However, about every 5 to 10 layers a c-layer spacing of 15 Å is observed. (b) and (c) were taken with the c-axis normal to the electron beam. The resolution is limited by sample thickness. Compared to the 10-K material, the 85- and 110-K materials are much more anisotropic, and sections with dimensions perpendicular to the c direction thin enough for high-resolution imaging are difficult to find in the crushed powders.

B. $n=2$

The preparation of the $Bi_2Sr_2Ca_1Cu_2O_8$ phase from stoichiometric amounts of the oxides and carbonates results in a multiphase sample.[12] However, single-phase materials are obtained by firing (at 850 °C for two days) a mixture of nominal composition 4:3:3:4. Crystals of this phase have been grown using an excess of Bi_2O_3 and CuO which, at these temperatures, act as a flux. The x-ray diffraction pattern of a plateletlike crystal is shown in Fig. 1(b). The [00l] reflections, which can be used as a signature, are shifted towards lower angles indicating a larger c axis than for the $n=1$ phase. Single-crystal x-ray studies[12] show a pseudotetragonal substructure with $a=5.39$ Å and $c=30.6$ Å. The TEM image in Fig. 3(b) shows the c axis repeat distance of $c/2=15.0$ Å. The structure contains one Ca layer sandwiched between two Cu-O_2, two Sr-O, and the two Bi-O layers resulting in $n=2$. As with the $n=1$ material, there is also a superstructure along the [0k0] direction. Single-crystal x-ray studies suggest that the $n=2$ phase has the chemical formula 4:4:2:4, whereas only compounds close to the nominal composition 4:3:3:4 are single phase. This result remains an enigma.

Another set of samples (M) of nominal composition 4:3:3:4 was prepared by melting the mixture (oxides plus carbonates) at 1140 °C and then cooling to 890 °C, whereupon it was maintained at this temperature for a few days before cooling to room temperature. The resulting samples contain plateletlike crystals (corresponding to the $n=2$ phase) embedded in a material which contains a few precent of second phase as determined by x-ray diffraction. These crystals have lattice parameters which are identical to those of the powdered samples, but they exhibit a different T_c, as discussed in Sec. III.

C. $n=3$

Mixtures of nominal composition 4:3:3:4 were rapidly raised to temperatures close to, but below, the melting point of the 4:3:3:4 phase (885 °C) and maintained at this temperature for about a week, then furnace cooled (6 h). After such a heat treatment, the alumina crucible container had, at its center, a black sintered phase on the top of which were crystals of golden color surrounded by a yellowish phase, most likely resulting from the decomposition of the 4:3:3:4 phase. The bulk of the material had "crystals" with metallic luster. These crystals exhibit only intermediate-range order (cryptocrystalline). The degree of long-range order of the crystals changes with the processing treatment and may also differ between crystals belonging to the same batch. Polycrystals with long-range order and a 110-K transition have been isolated, chemically analyzed, and studied by x-ray diffraction and TEM. A cation concentration of 2:2:2:3, similar to the 125-K T_c thallium phase, was obtained by wet chemical analysis. The x-ray pattern for one of these "crystals" pressed onto a glass slide is shown in Fig. 1(c). Because of the strong preferential orientation, only the [00l] lines diffract. Figure 1 compares this diffraction pattern to those obtained using plateletlike crystals of the $n=1$ and $n=2$ phases. Note that the low-angle Bragg peak is again

shifted to lower angles thus indicating an even larger c axis. From a least-squares fit of the Bragg peaks the unit-cell parameters $a=5.39$ Å and $c=37.1$ Å are obtained. By analogy to the thallium phase the increase in the c axis results from an extra CuO_2 layer ($n=3$).

Moreover, the diffraction lines for the 2:2:2:3 phase, as shown in Fig. 1(c), are broad and they are not exactly at [00l] positions. This line distortion could result from the presence of stacking faults. Because of the possible importance of such faults on the superconducting properties, we present the details of our analysis characterizing the stacking faults. A least-squares fit of the lattice parameter c to the [00l] peaks of Fig. 1(c) gives a root-mean-squared deviation of 0.2° between the calculated and measured values of the Bragg angle 2θ, as compared to a value of 0.02° typical for our diffractometer. This shift and some of the broadening can be explained by stacking faults in the 2:2:2:3 structure, faults in which some layers of $Cu_3Ca_2O_6$ are replaced by layers of $Cu_2Ca_1O_4$ from the 2:2:1:2 structure. The effects of such faults on the x-ray powder pattern can be calculated using the analysis of Hendricks and Teller.[20] In these Bi-based oxides, most of the x-ray scattering is produced by the sandwiches of $Bi_2Sr_2O_4$; the Cu and Ca layers in between determine the spacing between these sandwiches, but add little extra scattering. Thus, we can use the simplest case in Ref. 20, scattering from identical layers having random spacings. Let F be the structure factor for the $Bi_2Sr_2O_4$ sandwich, and let u_2 and u_3 be the spacing between the centers of $Bi_2Sr_2O_4$ sandwiches separated by 2 or 3 Cu layers (and 1 or 2 Ca layers). The x-ray intensity I per sandwich is given by

$$I=|F|^2\frac{1-\langle e^{iku}\rangle\langle e^{-iku}\rangle}{1-\langle e^{iku}\rangle-\langle e^{-iku}\rangle+\langle e^{iku}\rangle\langle e^{-iku}\rangle}, \tag{1}$$

where k is the scattering vector, $k=(4\pi/\lambda)\sin\theta$, and θ is the Bragg angle. The average of a quantity such as $\langle e^{iku}\rangle$ is defined as

$$\langle e^{iku}\rangle=\sum_{j=2}^{3}p_j e^{ikuj}, \tag{2}$$

where p_j is the probability that a given adjacent pair of $Bi_2Sr_2O_4$ sandwiches is separated by j Cu layers. (For simplicity, we consider only $j=2$ and $j=3$.) Then Eq. (1) becomes

$$I=|F|^2\frac{1-p_2^2-p_3^2-2p_2p_3\cos[k(u_2-u_3)]}{1+p_2^2+p_3^2+2p_2p_3\cos[k(u_2-u_3)]-2p_2\cos(ku_2)-2p_3\cos(ku_3)}. \tag{3}$$

We consider the case where the compound is largely the 2:2:2:3 phase, so $p_3>p_2$. When p_2 is zero, I consists of δ functions located where the denominator of Eq. (3) goes to zero, at $ku_3=l\pi$, with l an even integer. When p_2 becomes nonzero, the peaks broaden and shift. The numerator varies slowly over a given peak, and so determines only the peak's amplitude. The denominator D determines the shape and position of a given [00l] peak. Let ϕ measure the difference of ku_3 from an even integer multiple of π, according to

$$\phi=ku_3-l\pi. \tag{4}$$

Then if ϕ is small (as it is in our case), the denominator D becomes

$$D=A\phi^2+B\phi+C, \tag{5}$$

where the coefficients are given by

$$\begin{aligned}A&=1-p_2-p_2(1-p_2)\cos(ku_2),\\ B&=2p_2(1-p_2)\sin(ku_2),\\ C&=2p_2^2(1-\cos(ku_2)).\end{aligned} \tag{6}$$

This describes a Lorentzian, centered at

$$\phi_0=-B/2, \tag{7}$$

and with a full width at half maximum given by

$$\Delta\phi=\sqrt{4AC-B^2}. \tag{8}$$

Both the width and position of the peaks depend on the amount of disorder p_2 and (through ku_2) on the position of the peaks of the 2:2:1:2 structure. Although we need the full expressions above for some of the lines, it is instructive to consider the limit where p_2 is small and where the [00l] peak of 2:2:2:3 is near a [00l'] peak of 2:2:1:2. If the nearest 2:2:1:2 peak is δ away from an integer value of π, so that $ku_2=l'\pi+\delta$, then from Eqs. (7) and (8) the peak of the 2:2:2:3 structure will be shifted by $p_2\delta$ and be broadened to a full width at half maximum $p_2\delta^2$. Thus the peaks that are closest to [00l'] peaks of the 2:2:1:2 phase are shifted and broadened the least, and the broadening should vary more strongly from one peak to another than the shift does.

Of the observed [00l] lines in Fig. 1(c), the lines that are closest to lines from 2:2:1:2 are the [0012] and [0024]; these should be the least broadened. The [0014] line should be most broadened. The broadening does not vary as dramatically as the above results suggest, implying other contributions to the widths of a peak. Thus we used the peak positions rather than their widths to estimate p_2. We used Eq. (7) for ϕ_0 to correct the observed peak positions for different values of p_2, and found that for $p_2=0.25$ the least-squares refinement of the c-lattice parameter gives the lowest standard deviation. (The rms deviation between calculated and observed angles drops to 0.026° from the value of 0.20° found for $p_2=0$.) The value of c for the pure 2:2:2:3 structure found this way is $c=37.08\pm0.02$ Å.

Figure 4 compares the observed and calculated peaks using our model. The arrows show where the peaks should be for $p_2=0$. The dotted lines are Lorentzians calculated from Eqs. (7) and (8). Note that the calculated peaks are in the correct positions, but are all too narrow. This can be mostly explained by the extra instrumental

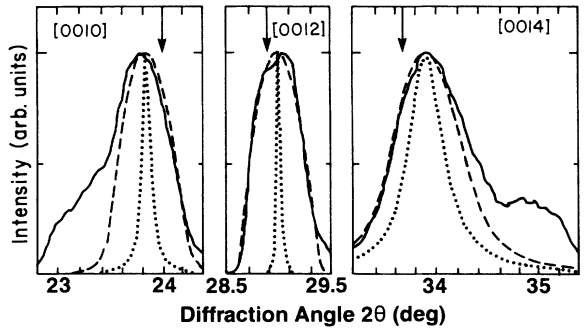

FIG. 4. Line shapes of the 2:2:2:3 compound, determined by x-ray powder diffraction, for three [00l] lines taken from the pattern shown in Fig. 1(c). The solid curves are the data (intensity measured in arbitrary units) with the baseline removed and with angles corrected for the displacement of the sample off the axis of the diffractometer. (This correction was determined during the least-squares refinement.) The arrows indicate where the Bragg peaks for a perfect 2:2:2:3 structure with $c=37.08$ Å would be. The dotted curves are Lorentzians whose positions and widths are calculated from Eqs. (7) and (8). The dashed curves are convolutions of the dotted curves with a parabolic line shape (see text). The extra peaks to the left of [0010] and to the right of [0014] are the [008] and [0012] peaks of the 2:2:1:2 structure.

broadening since we reduced the resolution of the instrument to give more intensity for this small sample. Thus, to account for this extra broadening, we convoluted the Lorenzian line shape with an arbitrary chosen parabolic line shape (defined as $I(\theta)=1-[(\theta-\theta_0)/\sigma]^2$ for $|\theta-\theta_0|<\sigma$ and 0 for $|\theta-\theta_0|>\sigma$; where I is the intensity, θ is the Bragg angle, θ_0 is the location of peak, and σ determines the width). The result of this simulation is displayed in Fig. 4 (dashed curve). In this figure, $\sigma=0.2$ for all the peaks.

Part of the crystal used to perform the x-ray measurements was also used for TEM. Within the basal plane, simple square patterns without or with extra spots corresponding to the modulation were observed. Thus, it is difficult to make a definitive statement about whether or not the modulation exists for the 2:2:2:3 phase. A TEM micrograph [Fig. 3(c)] taken perpendicular to the [00l] direction shows a Bi-O repeat unit of about 19 Å corresponding to a c axis of $(2\times\cong 19)\cong 38$ Å because of the doubling of the unit cell due to the crystallographic shear in the Bi-O layers. This value of c agrees well with that (37.1 Å) determined by x rays. It is also important to note that some repeat units are shorter because of stacking faults (the double Bi-O layer repeat unit is separated by 2 instead of 3 CuO_2 layers). This observation is consistent with the conclusions from our x-ray diffraction analysis.

III. PROPERTIES OF THE $Bi_2Sr_2Ca_{n-1}Cu_nO_y$ PHASES

We report here physical measurements collected only on crystals, or highly crystalline composites, of the Bi phases with $n=1$, 2, and 3. Cryptocrystalline materials, samples of the 110-K phase, whose order is so short range so as to preclude a proper x-ray characterization are not discussed.

Resistivity measurements, as a function of temperature, were made at constant current in a standard four-probe configuration. Indium (Ag) solder or silver ink contacts were used. The crystals examined were usually of constant thickness but of poorly defined shape such that the absolute values of the resistivity have, potentially, a large error and cannot be used to characterize the quality of the crystals. Figure 5 shows data for the $n=1$, 2, and 3 Bi-based phases. For the $n=1$ sample the resistance decreases linearly from room temperature down to close to T_c, whereas for $n=2$ the range of temperature over which this linear behavior is observed is considerably smaller and extends only from 300 down to 150 K. Finally, this linear resistivity behavior in the temperature region above T_c is not obeyed for the $n=3$ phase up to 200 K. The negative curvature behavior above T_c is unusual and we are not aware of any explanation which would account for this observation. Thus, we believe that the microstructure of these materials (including the propensity to fault as n increases) may be responsible for this curvature. This is consistent with our data since the largest curvature is observed for the $n=3$ phase which contains the most stacking faults.

To ensure that these phases are bulk superconductors, we measured magnetization with a dc superconducting quantum interference device (SQUID) magnetometer. The measurements were performed on crystals similar to those used for the resistivity measurements. Magnetic data are shown in Fig. 6. From the magnetization values, without taking into account the demagnetization factor, Meissner values greater than 50% are obtained for both the 85- and 110-K phase. Such values are obtained routinely on our bulk polycrystalline samples as well. This is in contrast to the thallium phases where the Meissner effect does not exceed 25%–30%.[16] For the 10-K Bi-based phase, however, we obtain a much smaller value (10%).

The properties of the three Bi phases discussed thus far do not reflect the difficulties encountered in the synthesis of these materials, as we observe that (for all of these phases) T_c depends upon the thermal treatment or histo-

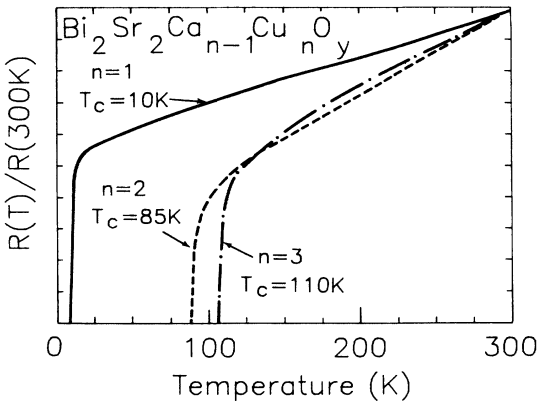

FIG. 5. The resistivity normalized to the resistivity at 300 K for crystals of $Bi_2Sr_2Ca_{n-1}Cu_nO_y$ with $n=1,2$, and 3 are shown.

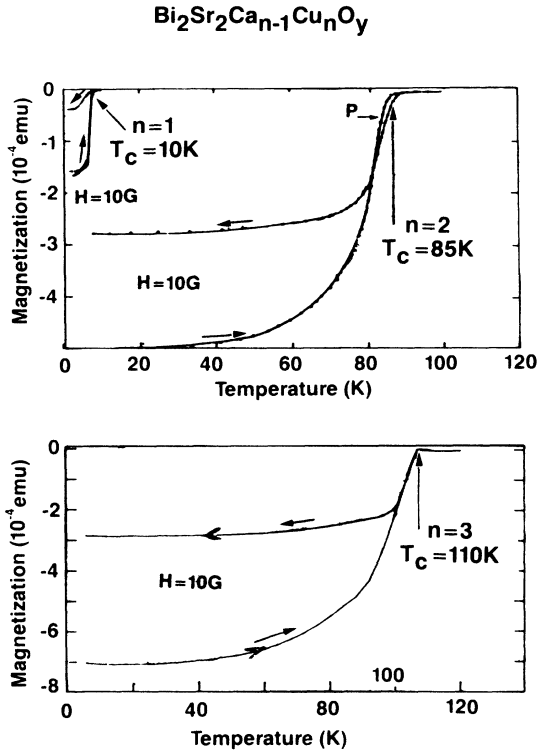

FIG. 6. The magnetization vs temperature for crystals of $Bi_2Sr_2Ca_{n-1}Cu_nO_y$ phases with $n=1$, 2, and 3 are shown. For each sample the upper curves are for cooling in a field of 10 G (Meissner) and the lower curves are for warming in a field of 10 G (shielding). According to the weight of the crystals a Meissner effect of 10%, 50%, and 50% was obtained for the $n=1$, 2, and 3 phases. These values have not been corrected for demagnetization effects.

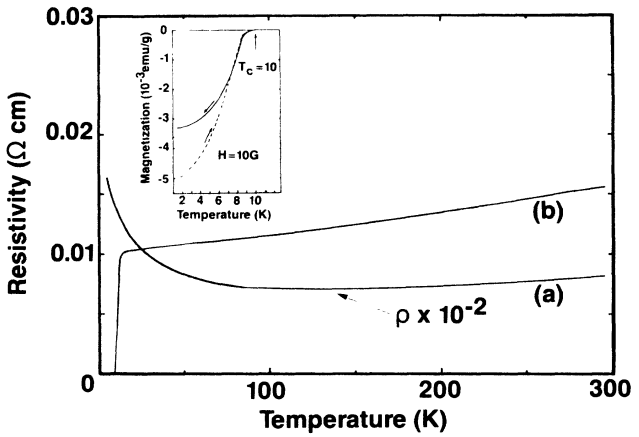

FIG. 7. The resistivity vs temperature from 4.2 up to 300 K is shown for samples of nominal composition 2:2:0:1 ($Bi_2Sr_2CuO_y$) heat treated differently. Sample (a) has been heated in sealed quartz ampoule at 870 °C for 15 h. Then a part of the same sample was fired at 895 °C for two extra hours (b). The inset shows the Meissner and shielding effects for the superconducting sample.

ry. We have studied this dependence in detail for the $n=1$ and $n=2$ phases. For $n=1$, the melted (M) samples are not superconducting; the sintered powder (P) samples show an increasing resistivity as T decreases, but then a superconducting transition at 10 K; and the Q samples (prepared in quartz) were semiconducting as prepared, but showed a superconducting transition and a metallic resistivity (decreasing with decreasing temperature) when they were annealed at 895 °C (Fig. 7). However, Fig. 7 shows that the Meissner effect in the superconducting sample is only about 5%, leaving some doubt about the existence of bulk superconductivity in this phase. The T_c's, as determined by ac susceptibility, for samples of nominal composition 4:3:3:4 but heat treated differently are shown in Fig. 8. Note that the thermal treatment can affect T_c by about 15 K with the highest T_c always associated with the melted (M) samples. Note also in Fig. 8 that T_c's as high as 94 K can be achieved.

It has been suggested[21] that T_c is related to the percentage of Cu(III) present in the material. There are several possibilities which could explain a large change in the formal valence of copper and thereby T_c. From previous work on the 1:2:3 compound, variations in oxygen stoichiometry might be expected to produce the observed changes in T_c. But, based on our earlier work on the Bi-based materials[12] we believe this is unlikely. A deficiency in the Bi content would lead to an increase in the average valence of copper which could produce a change in T_c. We performed a chemical analysis of several compounds of nominal composition 4:3:3:4 by means of volumetric titration using the Fe(II)/Fe(III) system as described elsewhere.[12] Although the samples exhibited different T_c's, or a mixture of 85 and 110 K, in all samples the same fraction (15%) of the Cu is detected as Cu(III) (within the accuracy of our measurements). A similar observation applies to the superconducting or nonsuperconducting 2:2:0:1 phase, both of which have the same amount of analyzed Cu(III).

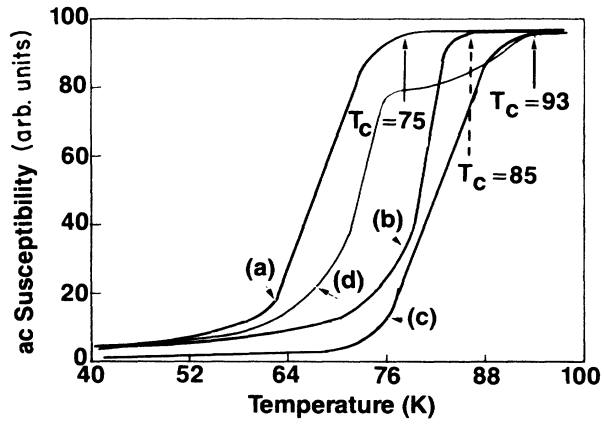

FIG. 8. Shown are the ac susceptibility vs temperature from 40 to 120 K for several samples of nominal composition 4:3:3:4 heat treated as follows. (a) Sample heated to 840 °C and slowly cooled. (b) Sample heated to 860 °C and slowly cooled. (c) Sample melted at 1140 °C, cooled in two hours to 890 °C and maintained at this temperature for three days prior to being quenched. (d) Sample treated as in (c) but slowly cooled.

We believe that the most likely possibility which accounts for the marked dependence of T_c on annealing temperature is the generation of stacking faults. The phases with $n=1$, 2, and 3 are the predominant phases in the Bi system, but stacking faults can exist in all of these phases. Such faults have the effect that, for phases of a given n, they produce a small amount of the $n+1$ or $n-1$ phases as defect regions. Thus the T_c of the resulting material will be either lowered from 85 K or increased depending upon the amount of $n-1$ (lower-T_c phase) or $n+1$ (higher-T_c phase). Above a critical concentration of stacking faults, both phases are present as a bulk in the sample, as shown in Fig. 8. The difference in thermodynamic free energy of these phases (which differ only by the number of stacking layers) is likely to be small. Thus, the removal of stacking faults is likely to be kinetically slow and, as with the layered materials, annealing temperature and cooling rate are important for growing the desired phase. For instance, we observe (Fig. 8) two different T_c traces for two parts of a sample treated simultaneously but then cooled in a different manner. The quenched sample shows a broad transition (10 K wide) whereas, over the same range of temperature, the slow-cooled sample shows unequivocally the presence of two superconducting phases. This observation indicates that the kinetics of the intergrowth formation are too slow to track the fast quenching rates.

IV. DISCUSSION

We have demonstrated the existence of three phases of general formula $Bi_2Sr_2Ca_{n-1}Cu_nO_y$ with $n=1$, 2, and 3 in the Bi-based system which are closely related from a structural point of view. Their pseudotetragonal structures (Fig. 9) can be described as a stacking of a basic $Bi_2Sr_2CuO_6$ unit with either zero, one, or two $CaCuO_2$ slabs inserted. The observed increase in the c lattice parameter from 24.6 to 30.6 and finally to 37.1 Å in going from the $n=1$ to $n=2$ and $n=3$ phases results from the progressive addition of 2×1 and 2×2 (doubled because of the crystallographic shear) $CaCuO_2$, each about 3-Å thick, to the stacking sequence in the unit cell. A similar increase in the c axis has also been observed with the thallium phases in going from $n=1$ to 2 and, finally, to 3. The complete structural picture for this series of compounds is more complicated than that shown in Fig. 9 because of a long-range modulation along the [010] direction, as was previously reported[12,13] for the $n=2$ phase. In contrast to the crystal chemistry of the thallium system, we are not able to synthesize Bi phases with only a monolayer of Bi-O (e.g., 1:2:2:3). Such a phase would have a shorter c axis than that for the $n=2$ phase and there would be a corresponding shift of the [00l] peaks to larger diffraction angles. In all the various Bi-based compositions we investigated, we never found evidence for such a phase.

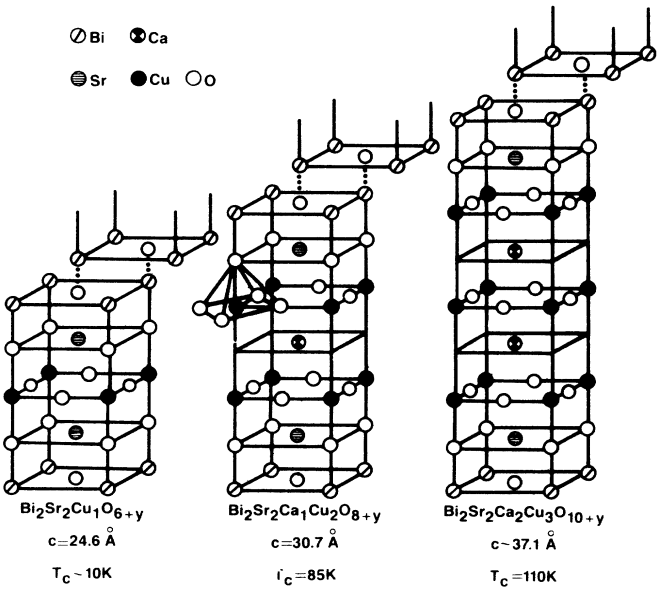

FIG. 9. The crystal substructures of the Bi phases of general formula $Bi_2Sr_2Ca_{n-1}Cu_nO_y$ with $n=1$, 2, and 3.

Common imperfections in layered materials are stacking alternatives and stacking faults. Such structural defects certainly affect some physical properties of the material, so that it is important to achieve a better characterization of the degree of stacking perfection. The difference in free energy between the various phases, which differ only in the numbers of $CaCuO_2$ slabs, is small so that stringent preparation conditions have to be established in order to minimize the occurrence of stacking faults or intergrowths. We believe these structural defects are responsible for the range of T_c's observed when, for instance, compounds of nominal composition 4:3:3:4 are treated differently. Changing the annealing temperature by only 10 °C is sufficient to change the T_c of the resulting material by 15 K. In general, a higher annealing temperature produces a higher T_c, but higher temperatures also increase the risk that one constituent, probably Bi, could be lost. Such a loss permits other stacking alternatives.

Based on studies of the $YBa_2Cu_3O_{7-x}$ phase, it could be concluded that the presence of Cu-O chains was necessary for obtaining the highest T_c's among the cuprate oxides. The present work on the Bi compounds, as well as similar work on the high-T_c thallium phases, whose structures also do not contain Cu-O chains, indicates that superconductivity resides in the CuO_2 planes. A similar conclusion was drawn from doping experiments on the 1:2:3 material where it was found that any substitution at the Cu site in the CuO_2 planes depressed T_c faster than any substitution at the Cu site belonging to a chain.[22-24] We believe that the double Bi-O layers in these new phases play the same role as the Cu-O chains in the 1:2:3 phase in that they act as a reservoir of holes. With the 1:2:3 compound the number of holes is easily changed by the addition or removal of oxygen. With the Bi-based phases it is more difficult to change the number of holes because it is more difficult to change the oxygen content. A deficiency in Bi can also generate holes on these layers. However, our attempts to dope the $n=2$ and $n=3$ materials, by changing either the oxygen or bismuth contents, resulted in the disintegration of the structure.

A feature common to the other high-T_c oxides is that they have closely related "parent" compounds that are antiferromagnetic insulators. For example, antiferromagnetism has been observed in insulating La_2CuO_4 (Ref. 25) and in $YBa_2Cu_3O_6$ (Ref. 26). For these new high-T_c compounds, based on Bi or Tl, the insulating regime is difficult to achieve. We have shown, however, that for the Bi phase with $n=1$ one can (depending on the synthesis temperature) obtain either semiconducting or superconducting behavior. Neutron studies on this material should indicate whether or not the same mechanism pertains to the Bi or Tl phases.

With every new class of superconducting oxides, one would like to establish systematics in the variation of T_c with composition so that higher T_c's can be found and so that the physics involved can be better understood. There have been correlations of T_c with the number of CuO_2 layers, indicating an increase in T_c of 30 K per addition of one CuO_2 layer.[15,27] This relation may hold for the thallium series but fails for the Bi series since T_c increases by 70 K as n goes from 1 to 2. In all the high-T_c cuprate oxides, the formal valence of Cu is greater than 2 and it has been suggested,[21] based on the 40- and 90-K materials (with various oxygen contents), that T_c scales linearly with the amount of +3 copper. This relationship is not confirmed for the 85-K Bi phase where an average Cu valence of 2.15 ± 0.02 has been determined. Furthermore, we show no detectable change in the Cu valence between the 85- and 110-K phases or between the $n=1$ phase in its superconducting and nonsuperconducting states. Hall measurements on defect-free single crystals would be of value in determining if the number of carriers scales with T_c.

ACKNOWLEDGMENTS

We thank B. Meagher, P. F. Miceli, P. Morris, J. M. Rowell, and J. H. Wernick for valuable discussions. M. A. Maedema and V. J. Boyko performed the spectrophotometric analysis.

[1]J. G. Bednorz and K. A. Müller, Z. Phys. B **64**, 189 (1986).
[2]M. K. Wu, J. R. Ashburn, C. J. Torng, P. H. Hor, R. L. Meng, L. Gao, Z. J. Huang, Y. Q. Wang, and C. W. Chu, Phys. Rev. Lett. **58**, 908 (1987).
[3]C. Michel, M. Hervieu, M. M. Borel, A. Grandin, F. Deslandes, J. Provost, and B. Raveau, Z. Phys. B **68**, 421 (1987).
[4]H. Maeda, Y. Tanaka, M. Fukutumi, and T. Asano, Jpn. J. Appl. Phys. **27**, L209 (1988).
[5]H. W. Zandbergen, P. Groen, G. Van Tandeloo, J. van Landuyt, and S. Amelinckz, Solid State Commun. **66**, 397 (1988).
[6]J. L. Tallon, R. G. Buckley, P. W. Gilberd, M. R. Presland, E. W. M. Brown, M. E. Bowden, L. A. Christian, and R. Goguel, Nature (London) **333**, 153 (1988).
[7]E. Takayama-Muromachi, Y. Uchida, Y. Matsui, M. Onoda, and K. Kato, Jpn. J. Appl. Phys. **27**, L556 (1988).
[8]Y. Matsui *et al.*, Jpn. J. Appl. Phys. **27**, L827 (1988).
[9]Y. F. Yan, C. Z. Li, J. H. Wang, Y. C. Chang, Q. S. Yang, D. S. Hou, X. Chu, Z. H. Mai, H. Y. Zhang, D. N. Zheng, Y. M. Ni, S. L. Jia, D. H. Shen, and Z. X. Zhao, Mod. Phys. Lett. B **2**, 571 (1988).
[10]J. K. Liang, S. S. Xie, G. C. Che, J. Q. Huang, Y. L. Zhang, and Z. X. Zhao, Mod. Phys. Lett. B **2**, 483 (1988).
[11]M. Hervieu, C. Michel, B. Domengues, Y. Laligant, A. Lebail, G. Ferey, and B. Raveau, Mod. Phys. Lett. B **2**, 491 (1988).
[12]J. M. Tarascon, Y. LePage, P. Barboux, B. G. Bagley, L. H. Greene, W. R. McKinnon, G. W. Hull, M. Giroud, and D. M. Hwang, Phys. Rev. B **37**, 9382 (1988).
[13]S. A. Sunshine, T. Siegrest, L. F. Schneemeyer, D. W. Murphy, R. J. Cava, B. Batlogg, R. B. VanDover, R. M. Fleming, S. H. Glarum, S. Nakahara, R. Farrow, J. J. Krajewski, S. M. Zahurak, J. V. Waszczak, J. H. Marshall, P. Marsh, L. W. Rupp, and W. F. Peck, Phys. Rev. B **38**, 893 (1988).
[14]Z. Z. Sheng and A. M. Hermann, Nature (London) **332**, 55 (1988); **332**, 138 (1988).
[15]C. C. Torardi, M. A. Subramanian, J. C. Calabrese, J. Gopalakrishnan, K. J. Morrissey, T. R. Askew, R. B. Flippen, U. Chowdry, and A. W. Sleight, Science **240**, 631 (1988).
[16]S. S. P. Parkin, V. Y. Nazzal, R. Savoy, R. Beyers, and S. J. LaPlaca (unpublished).
[17]J. M. Tarascon, Y. LePage, L. H. Greene, B. G. Bagley, P. Barboux, D. M. Hwang, G. W. Hull, W. R. McKinnon, and M. Giroud, Phys. Rev. B **38**, 2504 (1988).
[18]J. B. Torrance, Y. Tokura, S. J. LaPlaca, T. C. Huang, R. J. Savoy, and A. I. Nazzal (unpublished).
[19]C. C. Torardi, M. A. Subramanian, J. C. Calabrese, J. Gopalakrishnan, E. M. McCarron, K. J. Morrissey, T. R. Askew, R. B. Flippen, U. Chowdry, and A. W.Sleight, Phys. Rev. B **38**, 225 (1988).
[20]S. Hendricks and E. Teller, J. Chem. Phys. **10**, 147 (1942).
[21]B. Raveau, Physica C **153–155**, 3 (1988).
[22]G. Xiao, M. Z. Cieplak, D. Musser, A. Gavrin, F. H. Streitz, C. L. Chien, J. H. Rhyne, and J. A. Gotaas, Nature (London) **332**, 238 (1988).
[23]Y. Maeno, T. Tomita, M. Kyogoku, S. Awaji, Y. Aoki, K. Hoshino, A. Minami, and T. Fujita, Nature (London) **328**, 512 (1987).
[24]J. M. Tarascon, P. Barboux, P. F. Miceli, L. H. Greene, G. W. Hull, M. Eibschutz, and S. A. Sunshine, Phys. Rev. B **37**, 7458 (1988).
[25]D. Vaknin, S. K. Sinha, D. E. Moncton, D. C. Johnston, J. Newman, C. R. Safinya, and H. E. King, Jr., Phys. Rev. Lett. **58**, 2802 (1987).
[26]J. M. Tranquada, D. E. Cox, W. Kunnmann, H. Moudden, G. Shirane, M. Suenaga, P. Zolliker, D. Vaknin, S. K. Sinha, M. S. Alvarez, A. J. Jacobson, and D. C. Johnston, Phys. Rev. Lett. **60**, 156 (1988).
[27]P. Grant, Physica C **153–155**, 590 (1988).

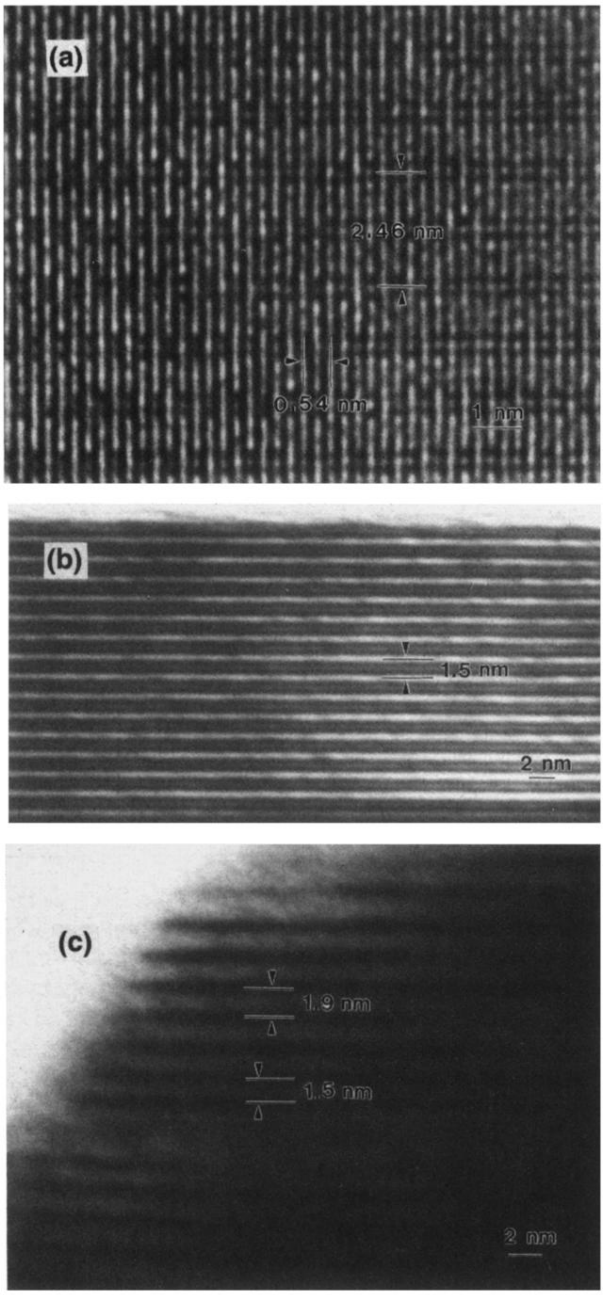

FIG. 3. Crushed powders of the three types of samples were examined using a JEOL 4000FX transmission electron microscope. (a) TEM lattice image of the 10-K material along the [100] direction. The double dark layers are assigned as the double Bi-O layers. The doubling of the unit cell due to the shearing of the Bi layers is delineated by the interweaving appearance of this micrograph. (b) Bright-field TEM image of the 85-K material showing uniform c-layer spacing of 15.4 Å. (c) Bright-field TEM image of the 110-K material showing imperfect order in the c direction. The observed c-layer spacing is usually 19 Å. However, about every 5 to 10 layers a c-layer spacing of 15 Å is observed. (b) and (c) were taken with the c-axis normal to the electron beam. The resolution is limited by sample thickness. Compared to the 10-K material, the 85- and 110-K materials are much more anisotropic, and sections with dimensions perpendicular to the c direction thin enough for high-resolution imaging are difficult to find in the crushed powders.